

New Limits on the Ultra-high Energy Cosmic Neutrino Flux from the ANITA Experiment

P. W. Gorham¹, P. Allison¹, S. W. Barwick², J. J. Beatty³, D. Z. Besson⁴, W. R. Binns⁵, C. Chen¹², P. Chen⁶, J. M. Clem⁷, A. Connolly¹¹, P. F. Dowkontt⁵, M. A. DuVernois⁹, R. C. Field⁶, D. Goldstein², A. Goodhue⁸, C. Hast⁶, C. L. Hebert¹, S. Hoover⁸, M. H. Israel⁵, J. Kowalski¹, J. G. Learned¹, K. M. Liewer¹⁰, J. T. Link^{1,13}, E. Lusczek⁹, S. Matsuno¹, B. C. Mercurio³, C. Miki¹, P. Miočinić¹, J. Nam^{2,12}, C. J. Naudet¹⁰, J. Ng⁶, R. J. Nichol¹¹, K. Palladino³, K. Reil⁶, A. Romero-Wolf¹, M. Rosen¹, L. Ruckman¹, D. Saltzberg⁸, D. Seckel⁷, G. S. Varner¹, D. Walz⁶, Y. Wang¹², F. Wu²¹

¹ Dept. of Physics and Astronomy, Univ. of Hawaii, Manoa, HI 96822. ² Dept. of Physics, Univ. of California, Irvine CA 92697. ³ Dept. of Physics, Ohio State Univ., Columbus, OH 43210. ⁴ Dept. of Physics and Astronomy, Univ. of Kansas, Lawrence, KS 66045. ⁵ Dept. of Physics, Washington Univ. in St. Louis, MO 63130. ⁶ Stanford Linear Accelerator Center, Menlo Park, CA, 94025. ⁷ Dept. of Physics, Univ. of Delaware, Newark, DE 19716. ⁸ Dept. of Physics and Astronomy, Univ. of California, Los Angeles, CA 90095. ⁹ School of Physics and Astronomy, Univ. of Minnesota, Minneapolis, MN 55455. ¹⁰ Jet Propulsion Laboratory, Pasadena, CA 91109. ¹¹ Dept. of Physics, University College London, London, United Kingdom. ¹² Dept. of Physics, Grad. Inst. of Astrophys., & Leung Center for Cosmology and Particle Astrophysics, National Taiwan University, Taipei, Taiwan. ¹³ Currently at NASA Goddard Space Flight Center, Greenbelt, MD, 20771.

We report initial results of the first flight of the Antarctic Impulsive Transient Antenna (ANITA-1) 2006-2007 Long Duration Balloon flight, which searched for evidence of a diffuse flux of cosmic neutrinos above energies of $E_\nu \simeq 3 \times 10^{18}$ eV. ANITA-1 flew for 35 days looking for radio impulses due to the Askaryan effect in neutrino-induced electromagnetic showers within the Antarctic ice sheets. We report here on our initial analysis, which was performed as a blind search of the data. No neutrino candidates are seen, with no detected physics background. We set model-independent limits based on this result. Upper limits derived from our analysis rule out the highest cosmogenic neutrino models. In a background horizontal-polarization channel, we also detect six events consistent with radio impulses from ultra-high energy extensive air showers.

In all standard models for ultra-high energy cosmic ray (UHECR) propagation, their range is ultimately limited by the opacity of the cosmic microwave background radiation. The UHECR energy above which this becomes significant is about 6×10^{19} eV in the current epoch. This cuts off their travel beyond distances of order 50 Mpc as first noted by Greisen [1], and Zatsepin and Kuzmin [2] (GZK). As a result of this absorption, the UHECR energy above this GZK cutoff is ultimately converted to photons, neutrinos, and lower energy hadrons. The resulting neutrinos were first described by Berezhinsky and Zatsepin (BZ) [3]. In standard UHECR source models the BZ neutrino fluxes peak at energies about 2 orders of magnitude below the GZK energy. Thus a “guaranteed” flux of neutrinos at energies of $E_\nu = 10^{17-20}$ eV exists. Its detection is one of the clearest ways to reveal the nature and cosmic distribution of the UHECR sources [4], which is one of the longest-standing problems in high energy astrophysics.

The ANITA-1 Long Duration Balloon experiment was designed specifically to search for this cosmogenic BZ neutrino flux. ANITA-1 exploits the Askaryan effect, in which strong coherent radio emission arises from electromagnetic showers in any dielectric medium [5]. The effect was first observed in 2000 [6], and has now been clearly confirmed and characterized for ice as the medium, as part of the pre-flight calibration of the ANITA-1 payload [7]. A prior flight of a prototype payload called ANITA-lite in 2003-2004 led to validation of the

technique and initial neutrino flux limits that ruled out several UHE neutrino models [8].

In a previous paper [9], we describe in detail the ANITA-1 instrument, payload, and flight system. Reference [9] also includes details of the instrument performance during the flight, estimates of the overall sensitivity of the instrument to neutrino fluxes, and discussions of possible backgrounds. Because of the complexity of the flight system and methodology, we refer the reader to ref. [9] for more detail when necessary.

The ANITA-1 payload (Fig. 1) launched from Williams Field, Antarctica near McMurdo station, on December 15, 2006, and executed more than three circuits of the continent. The payload landed on the Antarctic plateau about 300 miles from Amundsen-Scott (South Pole) Station, after 35 days aloft. Anomalous stratospheric conditions led to a misalignment of the polar vortex for the 2006-2007 season, and as a result the ANITA-1 trajectory spent an unusually large fraction of the time over West Antarctica where the ice sheet is smaller and shallower. In addition, the payload field-of-view to the horizon (at a distance of about 650 km at typical altitudes of 35-37 km above mean sea level, or 33-35 km above the ice surface), often included the two largest occupied stations in Antarctica, McMurdo and Amundsen-Scott, and thus was subject to higher-than-expected levels of anthropogenic electromagnetic interference (EMI). Despite these effects, the payload accumulated a net exposure livetime of 17.3 days

with a mean ice depth in the field of view of 1.2 km, comparable to the attenuation length of the ice at sub-GHz radio frequencies [10]. ANITA-1 was thus able to synoptically view a volume of ice of $\sim 1.6 \text{ M km}^3$. Our volumetric acceptance to a diffuse neutrino flux, accounting for the small solid angle of acceptance for any given volume element, is several hundred km^3 water-equivalent steradians at $E_\nu \simeq 10^{19} \text{ eV}$ [9].

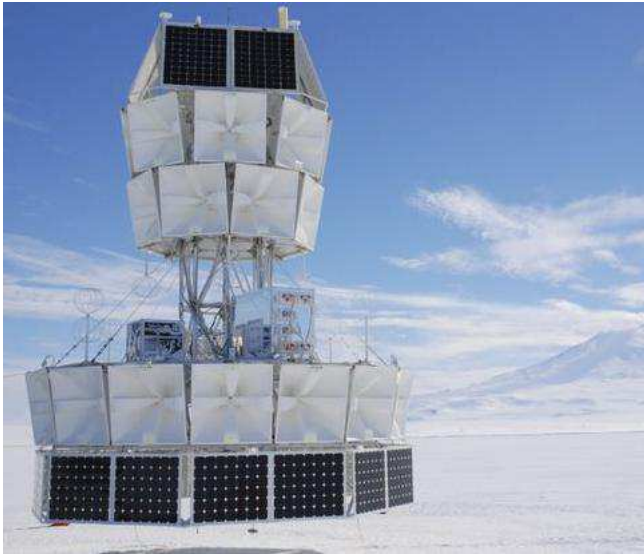


FIG. 1: View of the ANITA-1 payload in launch configuration, with photovoltaics at the top and bottom, and antenna clusters between. The side of each square antenna mouth is about 0.9 m, and the payload stands about 8 m tall.

ANITA-1’s antennas are 32 dual-linear-polarization, quad-ridged horns, each with a field of view which averages about 50° angular diameter over their 200-1200 MHz working bandwidth. The antennas are arranged in upper and lower rings, each with 16 antennas at azimuthal intervals of 22.5° . All antennas point at 10° below the horizontal, to maximize sensitivity to the largest portion of the volume near the horizon at 6° below the horizontal. The combined view of all antennas covers the entire lower hemisphere down to nadir angles of about 55° , comprising 99.4% of the area within the horizon. Radio impulses that exceed the ambient thermal noise by about 5σ in at least four antennas in coincident upper- and lower-ring pairs produce a trigger [9], and the entire antenna set of waveforms are then digitized and stored for later analysis. Thermal noise fluctuations produce random triggers at a rate of about 4-5 Hz, yielding a continuous monitor of instrument health. These events are incoherent in phase and produce a completely negligible background to actual coherent radio impulses.

The event analysis is conceptually simple, but requires detailed calibration of the instrument to achieve good precision. In the results reported here, we accepted only events having at least six adjacent antennas with detectable signals. The six antenna signals are analyzed using a method of pulse-phase

interferometry to determine the best arrival direction of the radio impulse plane wave, and this direction and its associated uncertainty is then mapped onto the Antarctic ice surface by reference to onboard payload navigation instruments, with an angular precision of $0.2^\circ \times 0.8^\circ$ in elevation and azimuth [9].

TABLE I: Event totals vs. analysis cuts and estimated signal efficiencies for unblinded ANITA-1 data set.

Cut requirement	passed:	total	Hpol	Vpol	Efficiency
(0) Hardware-Triggered	$\sim 8.2\text{M}$
(1) Upcoming plane wave	32308	15997	16311	0.93	
(2) Impulsive broadband	19695	10095	9600	0.98	
(3) Isolated from other events	9	8	1	0.94	
(4) Isolated from camps	6	6	0	0.96	
(5) Vpol dominant	0	0	0	0.99	

To minimize bias, the analysis cuts were optimized on a 10% randomized sample of the entire data set, and the remaining 90% was blinded from the analysts until the cuts were fixed. The cuts proceed as follows: **(1)** Events that do not reconstruct to a coherent plane wave in arrival direction are rejected as random thermal noise; events that reconstruct from directions above the horizon are also rejected. **(2)** Events that reconstruct but have non-impulsive waveforms from relatively narrow-band sources ($\leq 100 \text{ MHz}$) are rejected. **(3)** Events that cluster with one another in source location to within reconstruction errors projected onto the ice, or 50 km radius, whichever is greater, are rejected. True source candidates must be single, isolated events. Note that this cut, and the “camp cut” that follows it, are largely but not completely redundant. **(4)** Events that coincide in source location with any known active or inactive station, camp, aircraft flight path, or expedition traverse path, to within reconstruction angular errors projected onto the ice, or 50 km radius, whichever is greater, are rejected as being associated with anthropogenic activity. Even inactive camps or those long-abandoned are considered a risk, since left-over equipment might serve as a site for charge accumulation and associated electromagnetic discharges which could be mistaken for signals. **(5)** Events whose radio waveforms are not predominantly vertically polarized (Vpol) are rejected because, from considerations of the Askaryan impulse generation process, and the Fresnel transmission through the ice surface, they cannot originate from a particle shower within the ice sheet. Conversely, strongly horizontally polarized (Hpol) events are likely to originate from above the ice from similar considerations.

Table I shows the results of the total event sample after unblinding, including the signal efficiency for each cut separately. The 10% initial sample is included in the totals. Note that the isolation cut (3) is the single most stringent criterion in rejecting impulsive events, and this shows that the vast majority of triggers are not single, isolated events. Signal efficiency in each case was tested with a simulated event sample injected

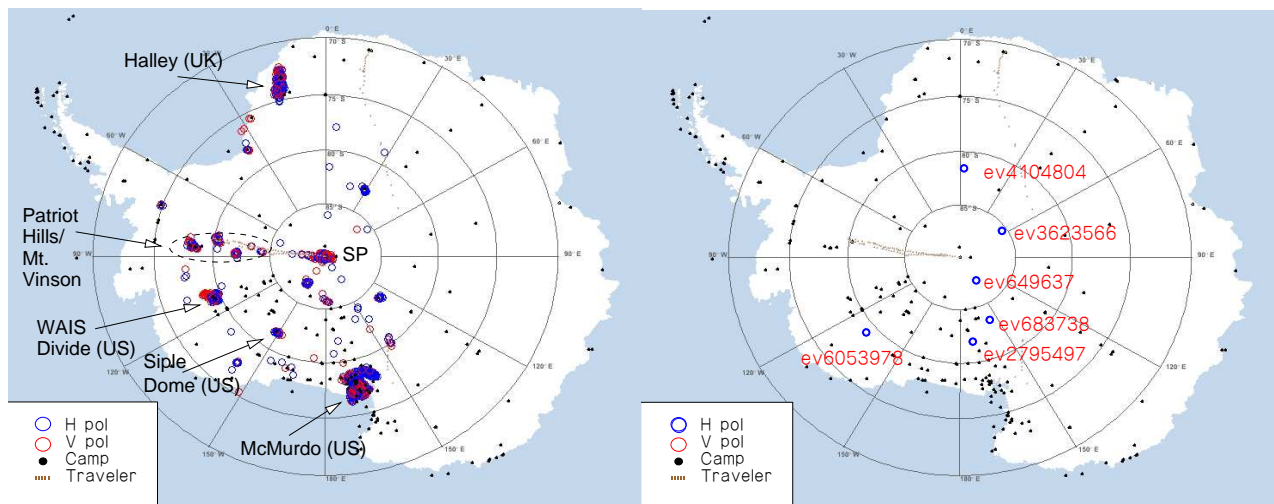


FIG. 2: Left: Plot of all reconstructed events, in both horizontal and vertical polarization; major Antarctic stations are indicated on the map. Right: events remaining after cuts to remove anthropogenic interference. 6 events remain in the horizontally polarized group, but these are non-candidates for neutrino events, as discussed in the text.

randomly into the data stream, and the final energy-averaged efficiency of all cuts is estimated to be 81%.

In Figure 2 we show the before-and-after maps of reconstructed ANITA-1 events superposed on the Antarctic continent. The strong correlation to a small number of stations is evident. The 6 surviving Hpol events are by contrast widely distributed across the continent, with no known camps or bases, either current or former, anywhere in their locale. We have investigated the possibility of impulsive signals from earth-orbiting satellites seen in reflection off the ice surface as a source for these events. This hypothesis is ruled out because the waveforms for these events do not show any evidence of differential group delay from ionospheric dispersion which is several ns per MHz in the 200-400 MHz frequency range where these events have most of their spectral power. In fact the signals are all of durations less than 10 ns. We know of no other anthropogenic sources for these events.

With regard to possible physics sources, our simulations of the high-frequency tail of impulsive geo-synchrotron radio emission [13, 14, 15] from ultra-high energy cosmic ray extensive air showers (EAS) suggest that these signals may be EAS events seen in reflection off the ice surface [9]. Such events are expected to be predominantly Hpol because of the strong Fresnel reflectivity in the region near Brewster's angle, and the overall initial preference for Hpol because of the more vertical polar magnetic fields. Our simulations predict a handful of such events for the flight, all of which arise from UHECR EAS with energies above 10^{19} eV; however, the uncertainties are large [9]. While these events do not constitute a background for our neutrino search because of their incorrect polarization, they are a potentially interesting signal in their own right. Further analysis, including a search for similar events from above the horizon, is in progress.

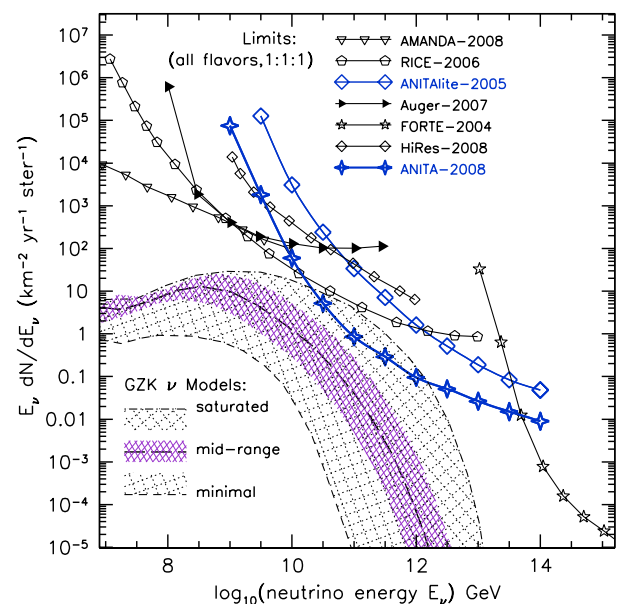


FIG. 3: ANITA-1 limits based on no surviving candidates for 18 days of livetime. Other limits are from AMANDA [16], RICE [17], ANITA-lite [8], Auger [18], HiRes [20], FORTE [19]. The BZ (GZK) neutrino model range is determined by a variety of models [11, 21, 23, 25, 26, 27, 29].

Based on the approach described in Refs. [19, 24], the resulting model-independent 90% CL limit on neutrino fluxes with Standard Model cross-sections [22] is shown in Fig. 3. Here we have included the net livetime and 81% analysis efficiency. Exclusion of the volume of ice near all camps and events reduces the net effective volume by a few percent. We

TABLE II: Expected numbers of events N_ν from several UHE neutrino models, and confidence level $CL = 100(1 - \exp(-N_\nu))$ for exclusion by ANITA-1 observations.

Model & references	predicted N_ν	CL,%
<i>Baseline BZ models</i>		
Protheroe & Johnson 1996 [21]	0.22	19.7
Engel, Seckel, Stanev 2001 [11]	0.12	11.3
Barger, Huber, & Marfatia 2006 [29]	0.38	31.6
<i>Strong source evolution BZ models</i>		
Engel, Seckel, Stanev 2001 [11]	0.39	32.3
Kalashov <i>et al.</i> 2002 [23]	1.03	64.3
Aramo <i>et al.</i> 2005 [26]	1.04	64.6
Barger, Huber, & Marfatia 2006 [29]	0.89	58.9
Yuksel & Kistler 2007 [28]	0.56	42.9
<i>BZ Models that saturate all bounds:</i>		
Kalashov <i>et al.</i> 2002 [23]	10.1	> 99.99
Aramo <i>et al.</i> 2005 [26]	8.50	> 99.98
<i>Waxman-Bahcall fluxes:</i>		
Waxman, Bahcall 1999, evolved sources [12]	0.76	53.2
Waxman, Bahcall 1999, standard [12]	0.27	23.7

estimate that experimental systematics such as variations in ice properties and calibration uncertainties in the absolute radio signal strength lead to uncertainties of order a factor of two on the limit. These model-independent limits are calibrated such that a model spectrum that matched the limit over one decade of energy would yield approximately 2.3 events; this choice is appropriate to smoothly varying models. The limits are an average over all three neutrino flavors, as ANITA-1 had roughly equal sensitivity to ν_e , ν_μ , ν_τ , and the flavors should be equally mixed to first order via oscillations for all BZ neutrino models. We plot only an approximate set of bands for the BZ neutrino models, which are too numerous to individually plot here.

In Table II we give the total number of events expected from selected individual ultra-high energy neutrino models which are representative of the range of BZ neutrino expectations; we also include the case of a model which saturates the canonical Waxman-Bahcall flux bounds for both evolved and standard UHECR sources [12]. ANITA-1 strongly limits the highest BZ neutrino models, which require extremely high-energy cutoffs in the parent cosmic-ray sources spectral energy distribution. Our limits thus suggest that UHECR source spectra extending to 10^{23} eV are disfavored. ANITA-1 sensitivity approaches a class of models here denoted as “strong-source evolution” models, which assume that the UHECR source evolution follows the cosmic evolution of more energetic sources, for example gamma-ray burst host galaxies [28]; these mid-range models are constrained at about the 60% CL but none are ruled out yet. The ANITA-1 90% CL integral flux limit on a pure E^{-2} spectrum for the energy range $10^{18.5} \text{ eV} \leq E_\nu \leq 10^{23.5} \text{ eV}$ is $E_\nu^2 F \leq 2 \times 10^{-7} \text{ GeV cm}^{-2} \text{ s}^{-1} \text{ sr}^{-1}$.

In summary, we have set the strongest bounds to date on the

ultra-high energy neutrino flux at energies above 3×10^{18} eV, using the radio Cherenkov method via synoptic observations of the Antarctic ice sheets from stratospheric altitudes. Our methodology appears to have no observed physics backgrounds, but may have detected events due to cosmic-ray extensive air showers that are easily separated from the neutrino events we seek.

This work has been supported by the National Aeronautics and Space Administration, the National Science Foundation Office of Polar Programs, the Department of Energy Office of Science High Energy Physics Division, and the UK Science and Technology Facilities Council. Special thanks to the staff of the Columbia Scientific Balloon Facility.

-
- [1] K. Greisen, Phys. Rev. Lett. 16, 748, (1966).
 - [2] G. T. Zatsepin, V. A. Kuzmin, JETP Lett. f 4, 78 (1966) [Pisma Zh. Eksp. Teor. Fiz. 4, 114, (1966)].
 - [3] V. S. Beresinsky, G. T. Zatsepin, Phys. Lett. B 28, 423 (1969).
 - [4] D. Seckel, T. Stanev, Phys. Rev. Lett. 95, 141101, (2005).
 - [5] G. A. Askaryan, JETP 14, 441, (1962); JETP 21, 658, (1965).
 - [6] D. Saltzberg *et al.*, Phys. Rev. Lett., 86, 2802, (2001).
 - [7] ANITA Collaboration: P. W. Gorham, *et al.*, Phys. Rev. Lett. 99, 171101, (2007).
 - [8] ANITA Collaboration: S. W. Barwick *et al.*, Phys. Rev. Lett. 96, 171101, (2006).
 - [9] ANITA Collaboration: P. W. Gorham, *et al.*, Phys. Rev. D, submitted 2008; arXiv:0812.1920.
 - [10] S. Barwick, D. Besson, P. Gorham, D. Saltzberg, J. Glaciol. 51, 231, (2005).
 - [11] R. Engel, D. Seckel, T. Stanev, Phys. Rev. D 64, 093010, (2001).
 - [12] E. Waxman, J. Bahcall, Phys. Rev. D 59, 023002, (1999).
 - [13] T. Huege, H. Falcke, Astropart. Phys. 24, 116, (2005); astro-ph/0501580.
 - [14] H. Falcke, P. Gorham, Astropart. Phys. 19, 477, (2003).
 - [15] D. A. Suprun, P. W. Gorham, J. L. Rosner, Astropart. Phys. 20, 157, (2003).
 - [16] IceCube Collaboration: M. Ackermann, *et al.* Astroph. Journ. 675:1014, (2008).
 - [17] I. Kravchenko, *et al.*, Phys.Rev. D 73, 082002, (2006).
 - [18] Pierre Auger Collaboration, Phys. Rev. Lett. 100, 211101, (2008).
 - [19] N. Lehtinen, P. Gorham, A. Jacobson, R. Roussel-Dupre, Phys. Rev. D 69, 013008, (2004); astro-ph/030965.
 - [20] HiRes Collaboration: R. U. Abbassi *et al.*, Ap. J. submitted, 2008; arXiv:0803.0554.
 - [21] R. J. Protheroe, P. A. Johnson, Astropart. Phys. 4, 253, (1996).
 - [22] R. Gandhi, Nucl. Phys. Proc. Suppl. 91, (2000) 453, (2000).
 - [23] O. E. Kalashev, V. A. Kuzmin, D. V. Semikoz, G. Sigl, Phys. Rev. D 66, 063004 (2002).
 - [24] L. A. Anchordoqui, J. L. Feng, H. Goldberg, A. D. Shapere, Phys. Rev. D 66, 103002, (2002).
 - [25] O. E. Kalashev, V. A. Kuzmin, D. V. Semikoz, G. Sigl, Phys. Rev. D 65, 103003, (2002).
 - [26] C. Aramo, *et al.*, Astropart.Phys. 23, 65, (2005).
 - [27] M. Ave, N. Busca, A. V. Olinto, A. A. Watson, T. Yamamoto, Astropart.Phys. 23, 19, (2005).
 - [28] H. Yuksel & M. D. Kistler, Phys. Rev. D 75, 083004, (2007) .
 - [29] V. Barger, P. Huber, D. Marfatia, Phys.Lett. B 642, 333, (2006).